SUPPORTING INFORMATION

Design and Synthesis of De Novo Boomerang Shaped Molecules and their *In Silico* & SERS-based Interactions with SARS-CoV-2 Spike Protein and ACE2

Amrutham Linet,[‡, a, b] Manu M. Joseph,[‡, a] Haritha Mambatta,[‡, a, b] K. Shamna,[a] Sunil Varughese,[a, b] P. Sujatha Devi,[*, a, b] C. H. Suresh,[*, a, b] Kaustabh Kumar Maiti,[*, a, b] Ishita Neogi[*, a, b]

[a] *Chemical Sciences and Technology Division, CSIR-NIIST, Thiruvananthapuram, Kerala, 695019, INDIA*

[b] *Academy of Scientific and Innovative Research (AcSIR), Ghaziabad, 201002*

kkmaiti@niist.res.in
ishita@niist.res.in
sureshch@niist.res.in
psujathadevi@niist.res.in

Table of Contents

General Aspects: All reactions were performed in oven-dried clean glassware. THF was distilled under a nitrogen atmosphere over sodium benzophenone ketyl. Dry Et_3N was prepared by storing over KOH before use. $PdCl_2(PPh_3)_2$, trimethylsilylacetylene were purchased from Spectrochem. Ethyl azidoacetate, Sodium L-ascorbate were purchased from TCI. Recombinant Human coronavirus SARS-CoV2 spike Glycoprotein S1 was purchased from Abcam (Cat no. ab273068) and ACE2 Protein, Human, Recombinant (Cat no. 10108-H08H) from Sino Biological Inc. All other commercially obtained solvents and chemicals were used without further purification. ^{1}H and ^{13}C NMR spectra were recorded on Brucker Avance III HD 500 spectrometers. The ESI mass spectra were recorded on Thermo scientific Exactive machine. IR spectra were recorded on Perkin Elmer FT-IR Instrument Spectrum. Figure 1(b) in the manuscript was drawn with the help of the Biovia Discovery studio visualizer. UV-vis absorption spectra were recorded using Shimadzu UV-vis Model UV-2600 spectrophotometer. PL studies were done using Flurolog Horiba Xe Lamp 450W spectrofluorometer.

Photophysical Studies: UV-vis absorbance of TBs were carried out in DMSO at a concentration of 10^{-5} M. Absorbance studies of ACE2 (0.5µg/mL), SARS-CoV-2 (0.33µg/mL), incubation of

TB-3 (0.5µg/mL) with SARS-CoV-2 spike protein (0.5µg/mL), incubation of TB-3 (0.5µg/mL) with ACE2 (0.5µg/mL), incubation of TB-3(0.45µg/mL) with SARS-CoV-2 (0.45µg/mL) and ACE2 (0.45µg/mL) were done in Milli-Q ultrapure water. Fluorescence emissions of TBs were done in DMSO at a concentration of 10^{-5} M (excitation wavelength used 270 nm).

Preparation of Stock Solution for Absorption studies: 1mg/mL stock solution of TB-3 was prepared in Milli-Q water, which was further diluted to 50 µg/mL. SARS-CoV-2 S-protein was commercially obtained from Abcam (Cat no. ab273068) in a solution state of concentration 200 µg/mL. From 200 µg/mL solution of S-protein, a sub-stock solution of concentration 50 µg/mL was prepared. Further, 250 µg/mL stock solution of ACE-2 was prepared in Milli-Q water, additional dilution offered a sub-stock solution of concentration 50 µg/mL. From these sub-stock solutions of concentration 50 µg/mL for TB-3, SARS-CoV-2, ACE-2 further dilutions were made for the absorption studies.

Molecular Docking: Micholas and Jeremy generated model of SARS-CoV-2 spike protein (NCBI Reference Sequence: YP_009724390.1) and ACE2 receptor (PDB: 2AJF) complex was used for molecular docking.[1] Optimized structure of TB1, TB-2, and TB-3 was obtained using Gaussian 09 at the M06L/6-311^{++}G** level of density functional theory (DFT). AutoDock 4.2 program package software was used for molecular docking. The Lamarckian genetic algorithm was applied to search for protein-ligand interaction.

Culture and maintenance of cell lines

Human cancer cell lines HeLa (cervical cancer) and A549 (lung adenocarcinoma) were obtained from the American-type Culture Collection (Manassas, USA). Human lung fibroblast cell line WI-38 was kindly gifted from IICB, Kolkata, India. Cells were maintained in Dulbecco's modified Eagle medium (DMEM) with 10% fetal bovine serum (FBS) and 5% CO_2 at 37 °C.

Cytotoxicity assay

The cytotoxicity of TB-1, TB-2, and TB-3 was evaluated over a wide range of concentrations for a period of 12 and 24 h using a clinically used chemotherapeutic agent doxorubicin (Dox) as a positive control. The cell growth inhibitory potential was measured using the 3-(4, 5-

dimethylthiazol-2-yl)2,5-diphenyltetrazoliumbromide (MTT) assay as described before.[2] Morphological changes were visualized under the phase contrast objective (Olympus 1 × 51, Singapore). Acridine orange-ethidium bromide dual staining was used for distinguishing viable and nonviable cells. The live/dead assays were performed as described previously[2] using TB-1, TB-2 and TB-3 (10 μg/mL) after 24 h incubation.

Tracking the molecular signature with label-free SERS fingerprinting

Surface-enhanced Raman spectroscopy (SERS) as an advanced modality of Raman spectroscopy was adopted and experiments were carried out with a confocal Raman microscope (WITec, Inc., Germany). Citrate stabilized gold nanoparticles (AuNPs) were used as a SERS substrate with a laser beam directed to the sample through 20×objective with a Peltier cooled CCD detector. The samples were excited with 633 nm laser (7 mW) to collect Stoke-shifted Raman spectra. Calibration was done with a silicon standard and data was processed using the WITec Project Plus (v2.1) software package, before each measurement. Raman spectra were collected, and the spectral variations upon treatment were accessed. We have employed colloidal spherical AuNPs within a size range of 40-45 nm emphasizing its best SERS activity. AuNPs were synthesized as per the standard method using the citrate reduction method and optimized size, shape, and mono-dispersity were confirmed.[3] We set up ~ 40-45 nm size AuNPs having plasmon peaks around 528 nm and colloidal concentration 8.8 x 1012 particles (100 μL) in order to assess the Raman fingerprinting. For the molecular interaction studies, recombinant human ACE-2 (10108-H08H, Sino Biological Inc. Beijing, China) and recombinant coronavirus SARS-CoV2 spike Glycoprotein S1 (ab273068, Abcam, USA) was used. An equal ratio of TB-3 (50 μg/mL), ACE-2 (50 μg/mL), and SARS-CoV-2 (50 μg/mL) were mixed and incubated for 1 h and SERS measurements were at rt made after mixing with AuNPs (20 μL). A minimum of 50 individual spectra from each group was subjected to principal component analysis (PCA) using the statistical toolbox of MATLAB 2015b (Mathworks, MA) to obtain principal component scores.

Scheme S1: Synthesis of TB-1, TB-2, and TB-3

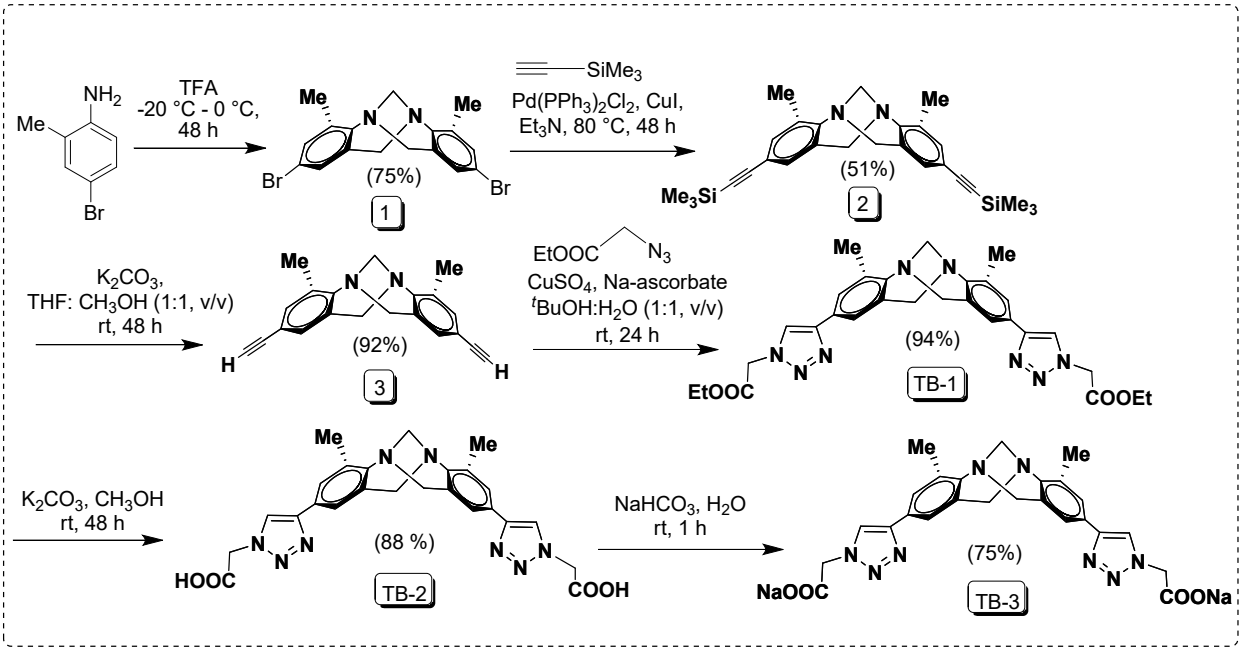

1. Synthesis of Compound 2

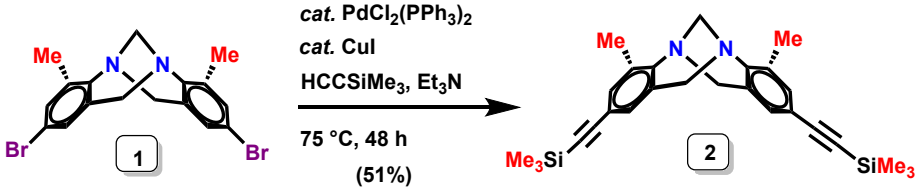

2,8-Dibromo-**TB** (**1**) was synthesized following the reported literature procedure.[4] To an oven-dried and N_2 purged pressure tube was added **1** (500 mg, 1.22 mmol) and CuI (10 mg, 0.05 mmol). Thereafter, the pressure tube was charged with dry Et_3N (10 mL), followed by trimethylsilylacetylene (0.5 mL, 3.18 mmol) and $PdCl_2(PPh_3)_2$ (48 mg, 0.06 mmol). All reagents were added under nitrogen atmosphere, thereafter the pressure tube was sealed and the reaction mixture was magnetically stirred with heating in an oil bath at 75 °C for 2 days. Next, the reaction mixture was washed with saturated $NaHCO_3$ and DCM. The organic layer collected was dried over anhydrous $NaSO_4$, filtered, and concentrated under vacuo. Silica-gel column chromatographic purification in hexane/EtOAc (95:5, v/v) gave required product **2** as a

colourless solid (274 mg, 51 % yield); **^{1}H NMR** ($CDCl_3$, 500 MHz): δ 7.15 (s, 2H), 6.89 (s, 2H), 4.50 (d, J = 16.8 Hz, 2H), 4.27 (s, 2H), 3.91 (d, J = 16.8 Hz, 2H), 2.33 (s, 6H), 0.19 (s, 18H).

2. Synthesis of Compound 3

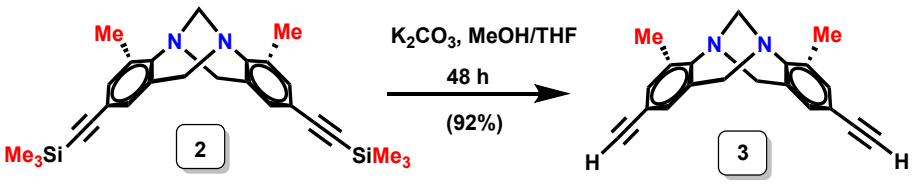

Compound **2** (100 mg, 0.22 mmol) was dissolved in 20 mL CH_3OH:THF (1:1, v/v), added K_2CO_3 (124.8 mg, 0.90 mmol) to it. The reaction mixture was stirred for 48 h at rt. Subsequently, solvent was removed under vacuo to get crude product of **3**. Reaction mixture was purified by column chromatographic using hexane/EtOAc (95:5, v/v) that gave pure colourless solid **3** (62 mg, 92 % yield); **^{1}H NMR** ($CDCl_3$, 500 MHz): δ 7.19 (s, 2H), 6.92 (s, 2H), 4.53 (d, J = 16.8 Hz, 2H), 4.27 (s, 2H), 3.94 (d, J = 16.9 Hz, 2H), 2.96 (s, 2H), 2.36 (s, 6H); **^{13}C NMR** ($CDCl_3$, 125 MHz): δ 146.64, 133.06, 132.65, 128.31, 128.06, 117.15, 83.55, 77.30, 77.04, 76.79, 76.25, 67.33, 54.72, 16.94. **ESI-HRMS**: Calcd for $C_{21}H_{19}N_2$ 299.1548 $[M+H]^+$, found 299.1539.

3. Synthesis of TB-1

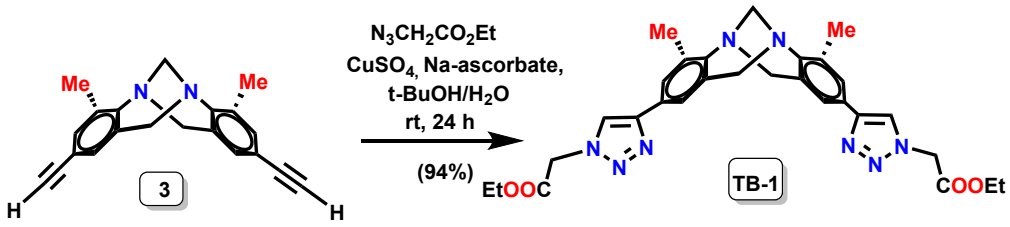

A mixture of *tert*-butyl alcohol and distilled water (6 mL, 1:1, v/v) was taken in a pressure tube, it was degassed and back filled with N_2 for three times. To it was added **3** (100 mg, 0.33 mmol), $CuSO_4 \cdot 5H_2O$ (8.40 mg, 0.03 mmol), sodium L-ascorbate (10 mg, 0.05 mmol) and ethyl azidoacetate (173 mg, 1.34 mmol). The pressure tube was sealed under nitrogen atmosphere and the reaction mixture was stirred for 24h at rt. After this period, solvent was removed under

vacuo, the crude was washed with ethyl acetate and distilled water several times to obtain compound **TB-1** as pure white solid (175.9 mg, 94 % yield). IR (solid) cm^{-1} 3138, 2978, 2898, 2846, 1752, 1581, 1465, 1441,1412,1397,1374,1346, 1327,1302,1284,1211,1066,1050, 1017; **^{1}H NMR** (DMSO-d_6, 500 MHz): δ 8.36 (s, 2H), 7.54 (s, 2H), 7.32 (s, 2H), 5.38 (s, 4H), 4.57 (d, J = 17 Hz, 2H), 4.28 (s, 2H), 4.16 (q, J = 7.1 Hz, 4H), 4.07 (d, J = 17 Hz, 2 H), 2.41 (s, 6H), 1.20 (t, J = 7.1 Hz, 6H); **^{13}C NMR** (DMSO-d_6, 125 MHz): δ 167.70, 146.80, 146.05, 133.39, 129.15, 126.04, 125.95, 122.56, 121.77, 67.46, 62.07, 54.87, 50.92,17.39, 14.39S; **ESI-HRMS**: m/z Calcd for $C_{29}H_{33}N_8O_4$ 557.2625 $[M+H]^+$, found 557.2648.

4. Synthesis of TB-2

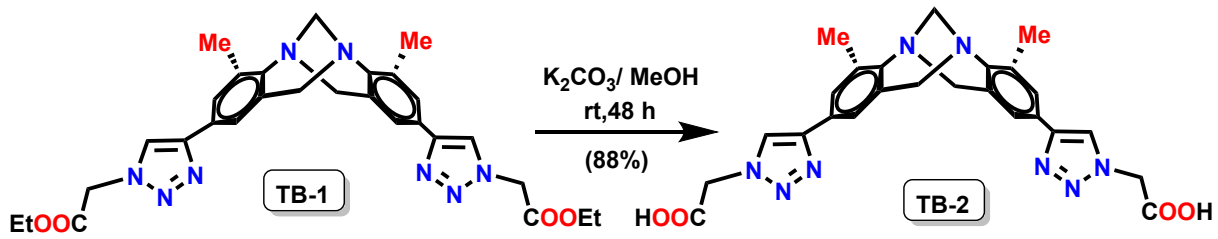

To a solution of **TB-1** (655 mg, 1.17 mmol) in CH_3OH (100 mL) was added K_2CO_3 (976 mg, 7.06 mmol), the mixture was stirred at room temperature for 48 h. After completion of reaction, solvent was removed under vacuo and the solid residue was dissolved in minimum amount of H_2O. The reaction mixture was placed in ice bath and neutralized with dropwise addition of 50% HCl addition continued until the mixture became acidic. Precipitated product was collected by filtration, washed thoroughly with distilled water and dried under vacuo to obtain pure solid **TB-2** (522 mg, 88 % yield). IR (solid) cm^{-1} 3234, 3122, 3088, 3008, 2957, 1706, 1612, 1449, 1426, 1383, 1344,1327, 1300, 1233, 1212, 1108, 1083, 1050, 1005; **^{1}HNMR** (DMSO-d_6, 500MHz): δ 8.35 (s, 2H), 7.54 (s, 2H), 7.32 (s, 2H), 5.27 (s, 4H), 4.58 (d, J = 17.0 Hz, 2H), 4.31 (s, 2H), 4.08 (d, J = 17.1 Hz, 2H), 2.42 (s, 6H); **^{13}C NMR** (DMSO-d_6,125 MHz): δ 169.24, 146.69, 145.78, 133.33, 129.03, 126.28, 126.09, 122.53, 121.78, 67.54, 54.91, 51.07, 17.38. **ESI-HRMS**: m/z Calcd for $C_{25}H_{25}N_8O_4$ 501.1998 $[M+H]^+$, found 501.2015.

5. Synthesis of TB-3

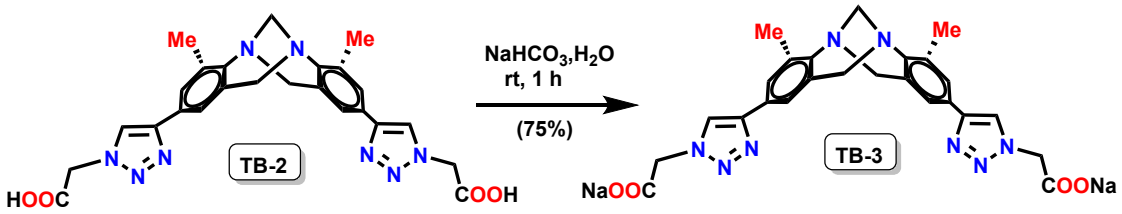

To a solution of **TB-2** (50 mg, 0.09 mmol) in deionised H_2O (4 mL) was added $NaHCO_3$ (17.6 mg, 0.20 mmol). The reaction was stirred at rt for 1h. After the bubbles of CO_2 ceased, the reaction mixture was lyophilized to obtain free flowing white solid particles of **TB-3** (40.76 mg, 75 % yield). IR (solid) cm^{-1} 3375, 3136, 2952, 2891, 2840, 1606, 1464, 1428, 1393, 1360, 1307, 1242, 1212, 1169, 1131, 1095, 1064, 1029, 1005; **^{1}H NMR** (CD_3OD, 500 MHz): δ 8.15 (s, 2H), 7.56 (s ,2H), 7.31 (s, 2H), 4.98 (s, 4H), 4.66 (d, J = 16.9 Hz, 2H), 4.39 (s, 2H), 4.14 (d, J = 16.9 Hz, 2H), 2.49 (s, 6H); **^{13}CNMR** (CD_3OD, 125 MHz): δ 170.79, 146.77, 145.85, 133.31, 128.68, 126.41, 126.07, 122.02, 121.51, 67.41, 54.90, 53.40, 16.33. **ESI-HRMS**: m/z Calcd for $C_{25}H_{23}N_8Na_2O_4$ 545.16376 $[M+H]^+$, found 545.16412.

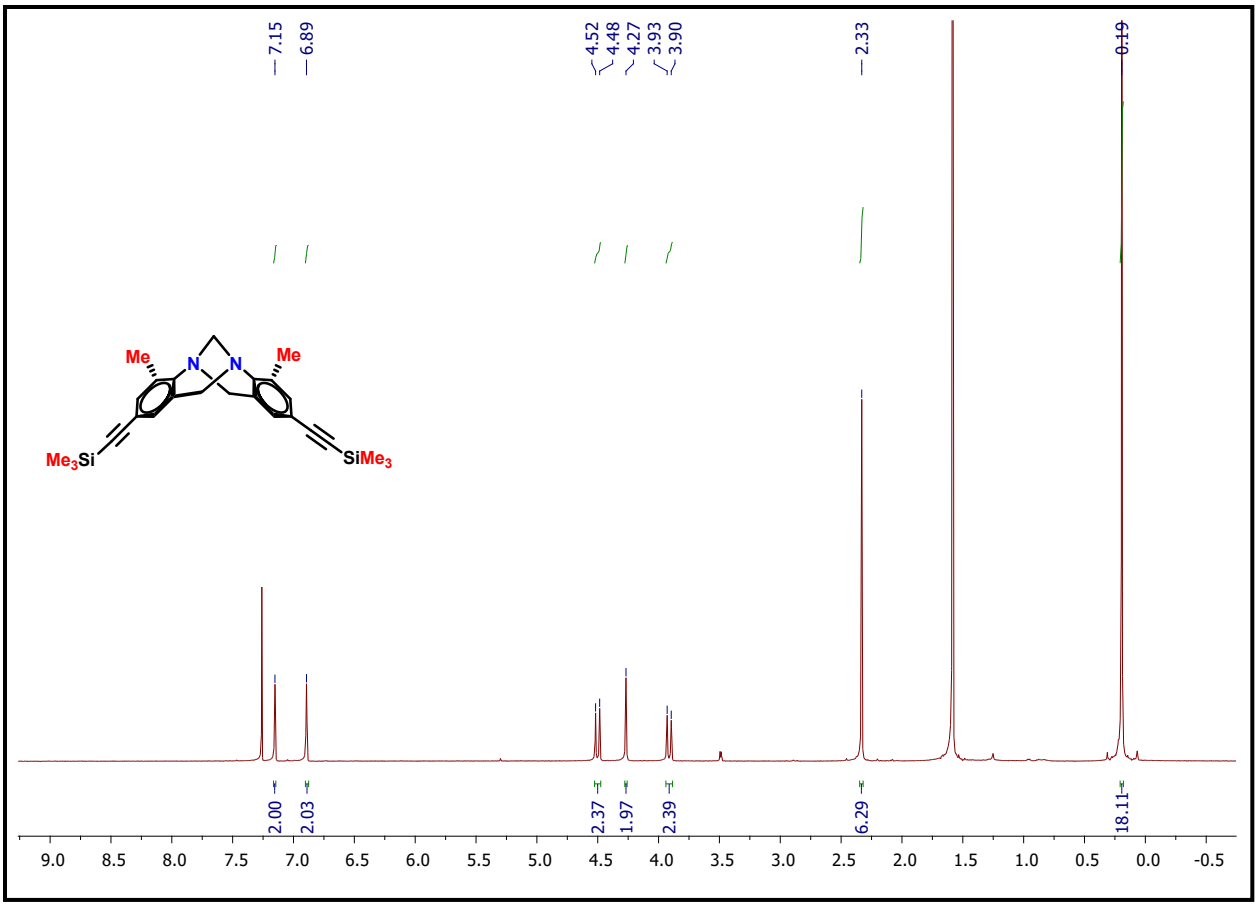

Figure S1. ^{1}H NMR spectrum (500 MHz, $CDCl_3$) of 2.

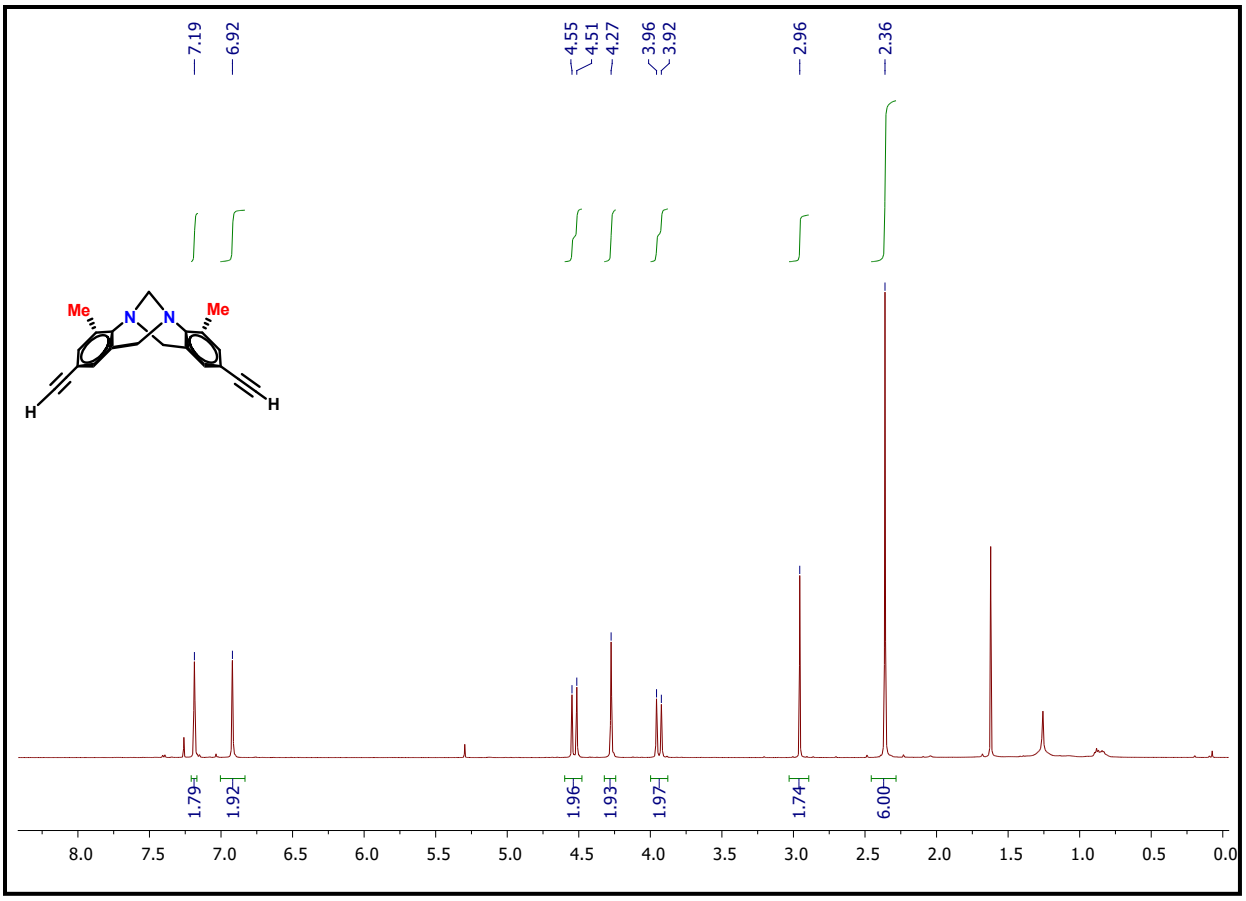

Figure S2. ^{1}H NMR spectrum (500 MHz, $CDCl_3$) of 3.

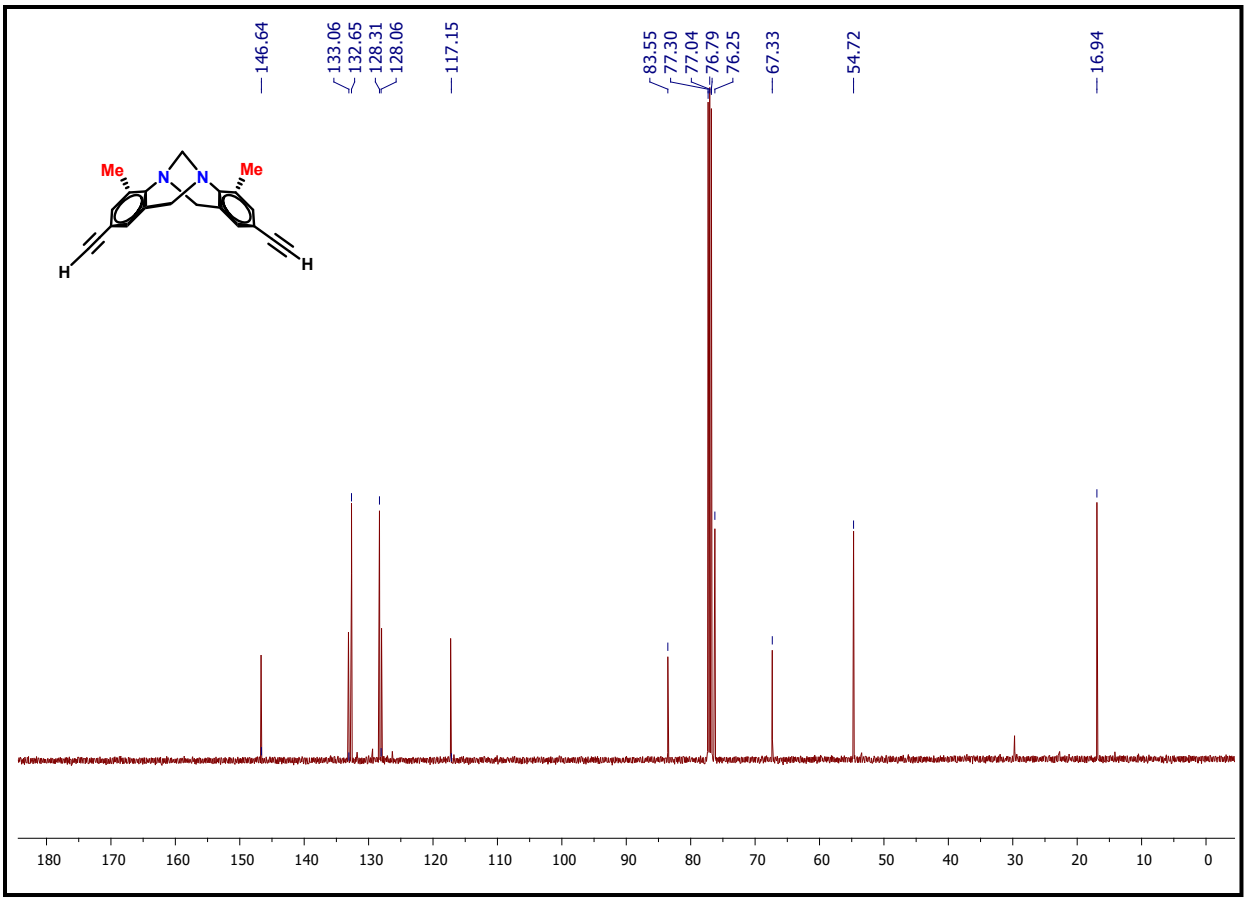

Figure S3. ^{13}C NMR spectrum (125 MHz, $CDCl_3$) of 3.

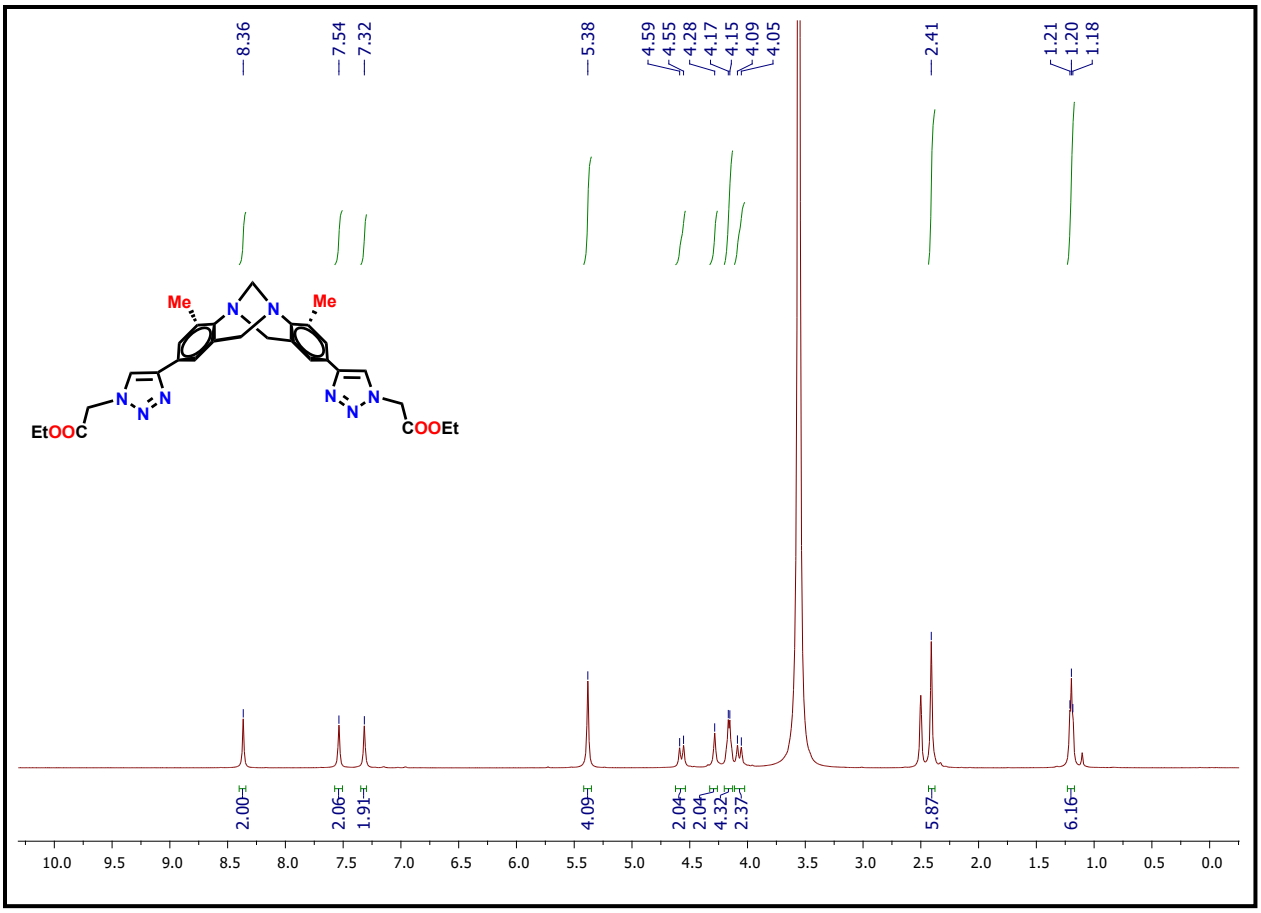

Figure S4. ^{1}H NMR spectrum (500 MHz, DMSO-d_6) of TB-1.

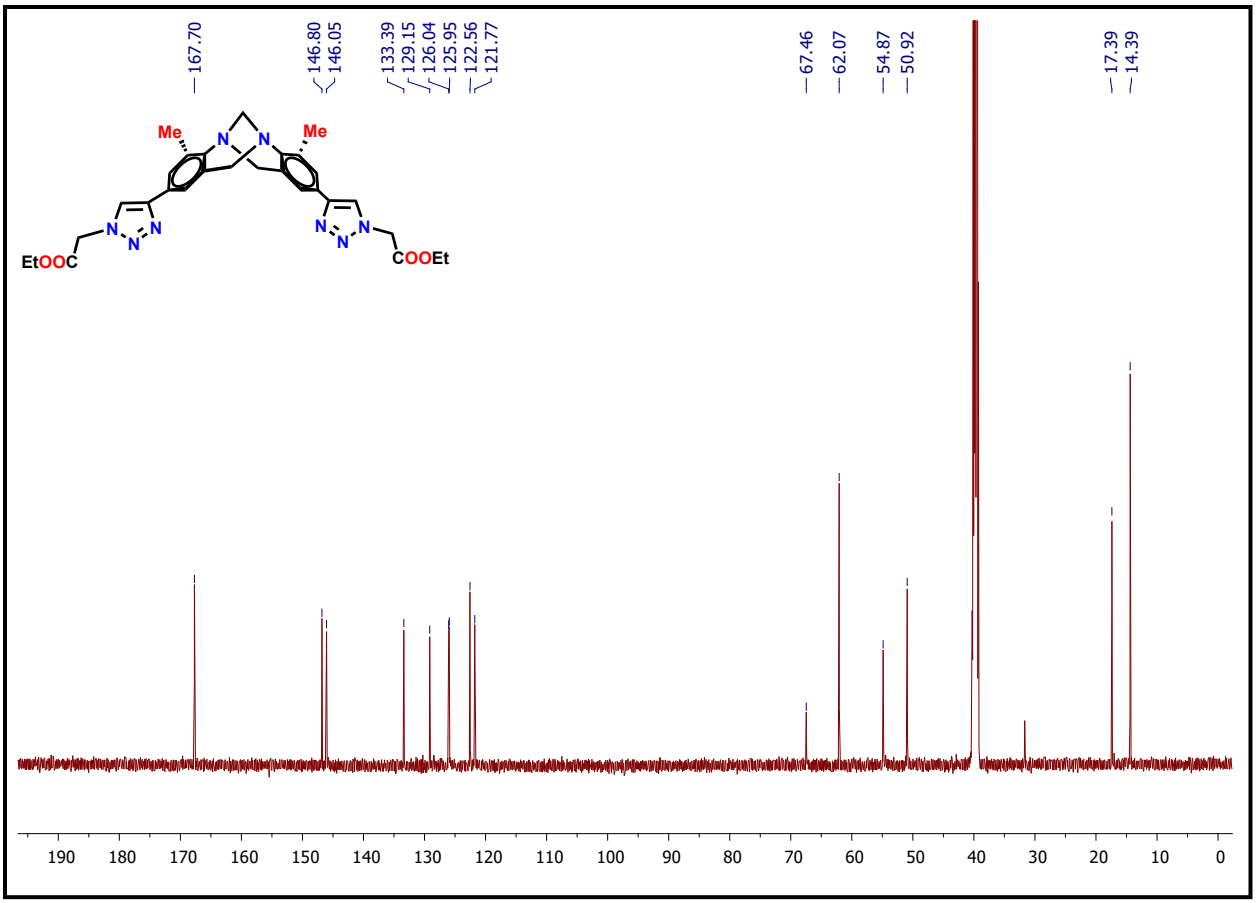

Figure S5. ^{13}C NMR spectrum (125 MHz, DMSO-d_6) of TB-1.

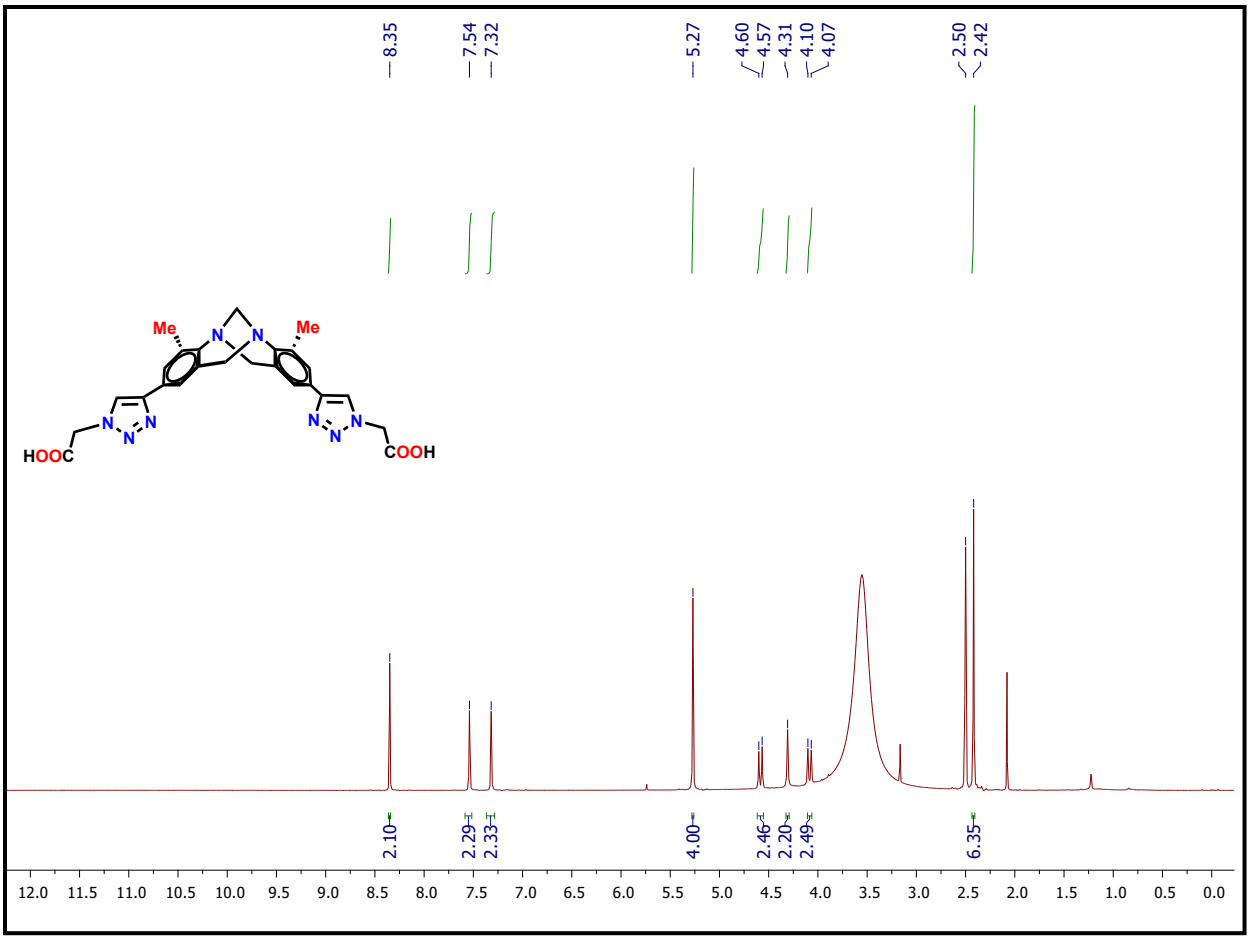

Figure S6. ^{1}H NMR spectrum (500 MHz, DMSO-d_6) of TB-2.

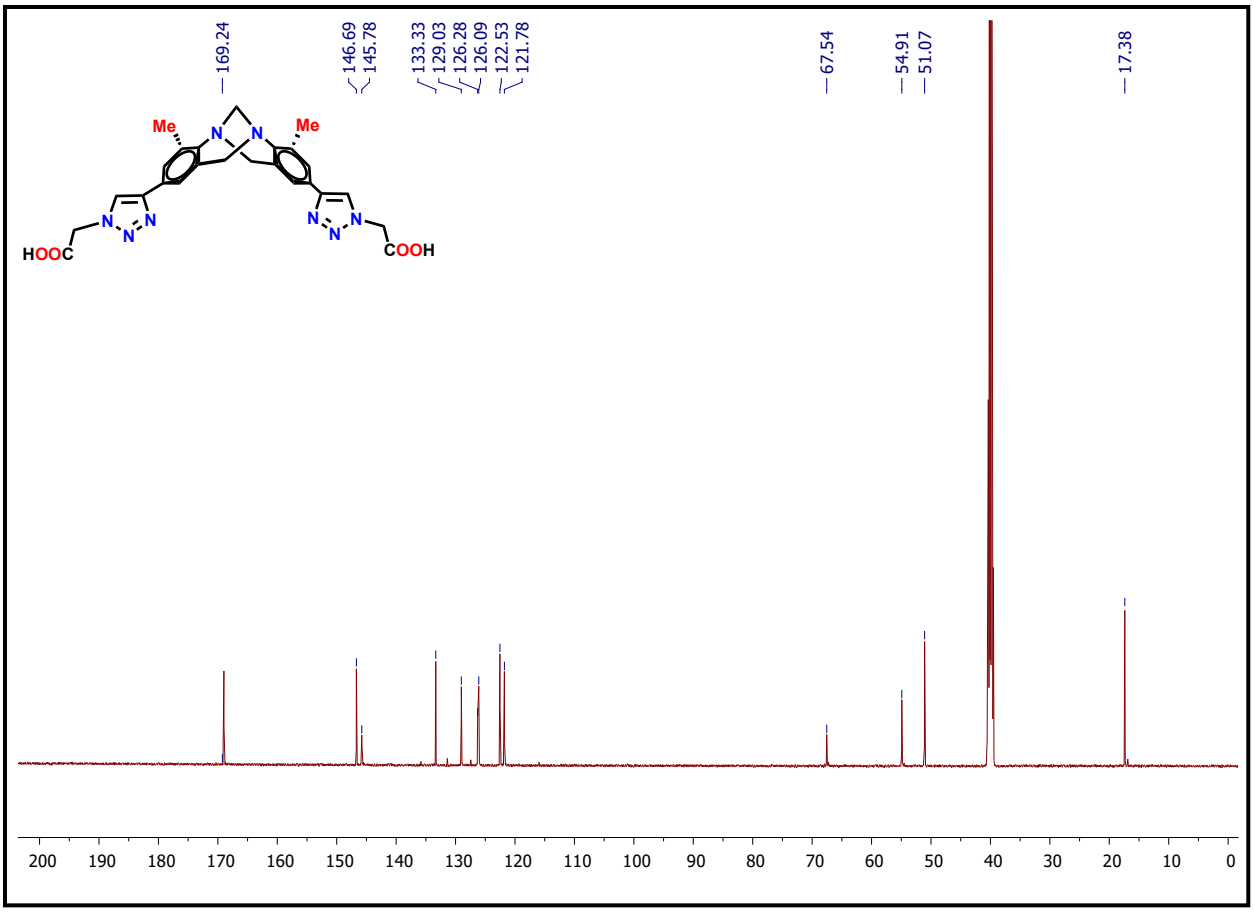

Figure S7. ^{13}C NMR spectrum (125 MHz, DMSO-d_6) of TB-2.

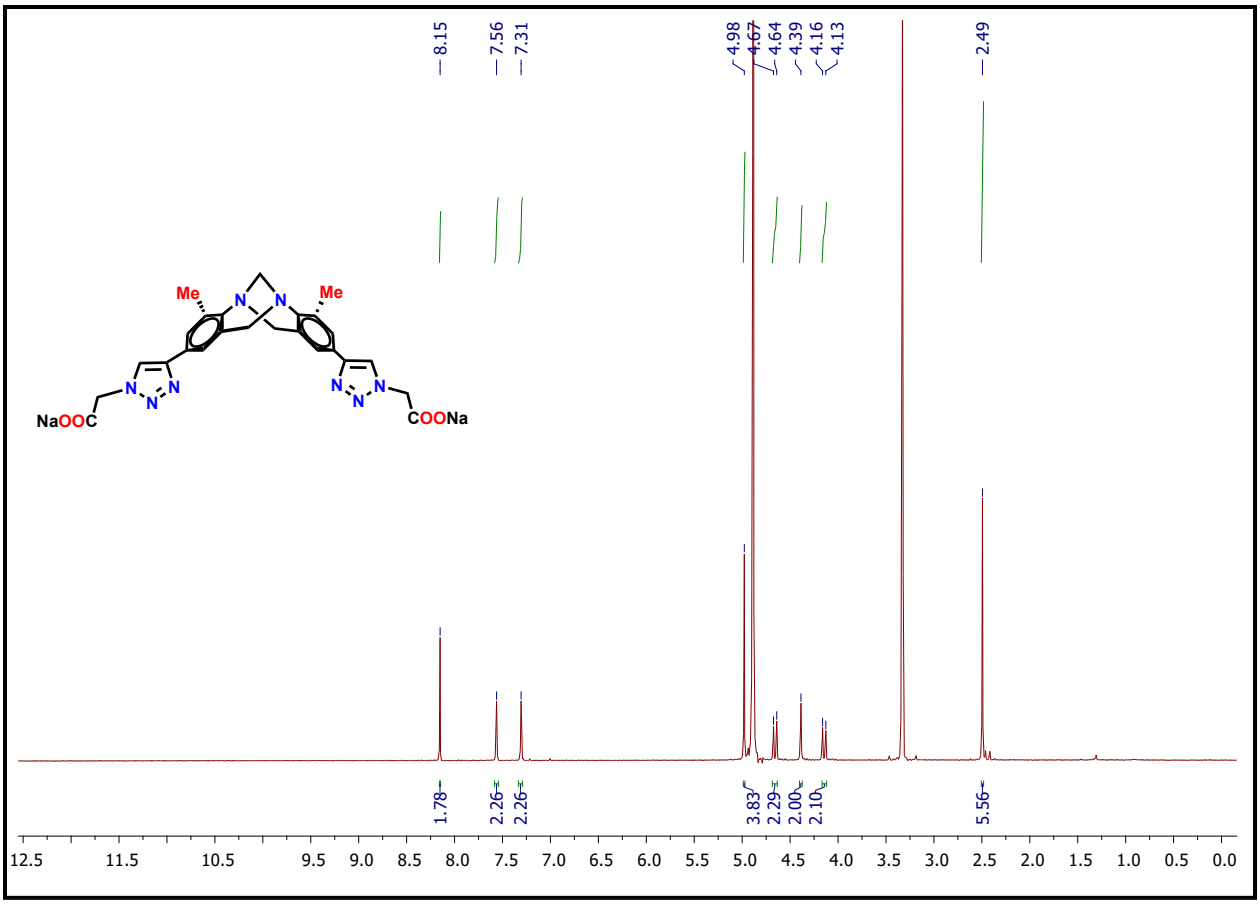

Figure S8. ^{1}H NMR spectrum (500 MHz, CD_3OD) of TB-3.

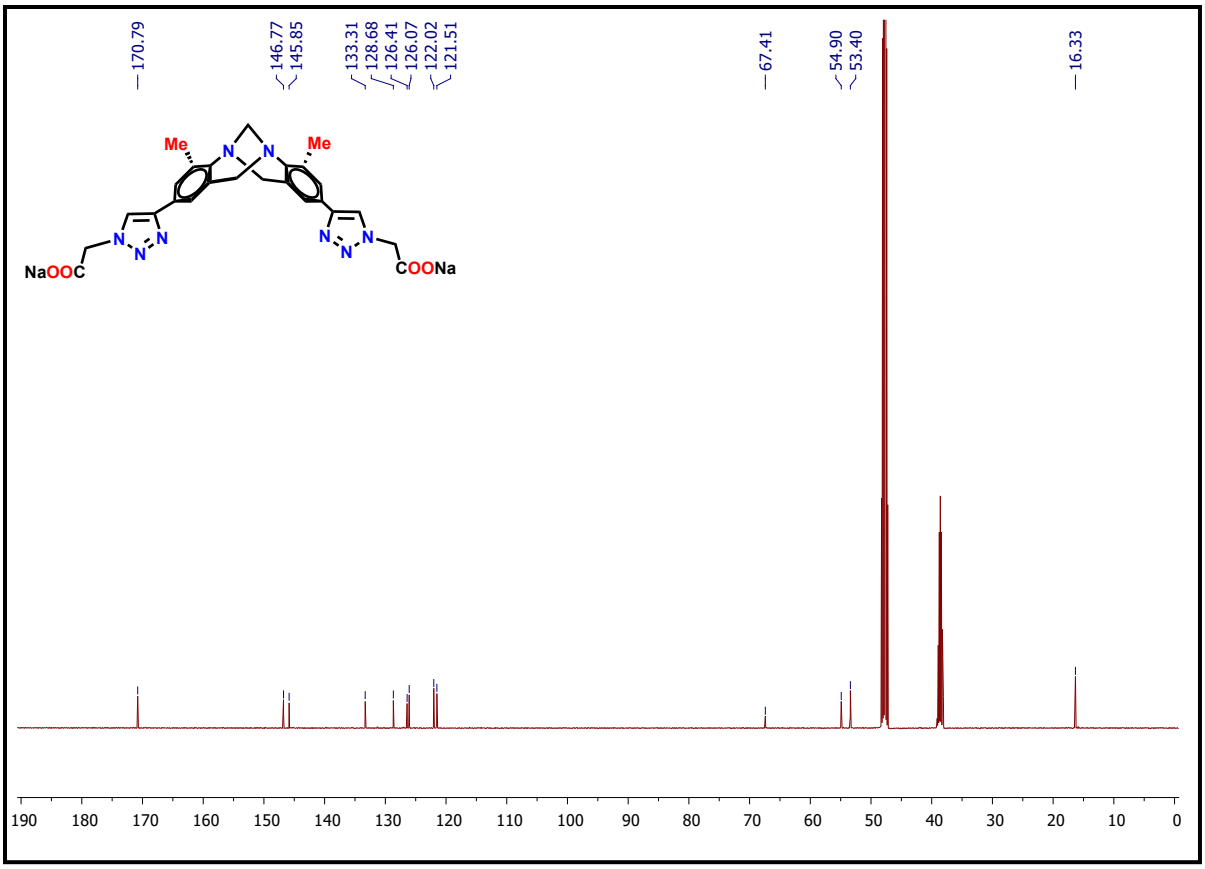

Figure S9. ^{13}C NMR spectrum (125 MHz, CD_3OD) of TB-3.

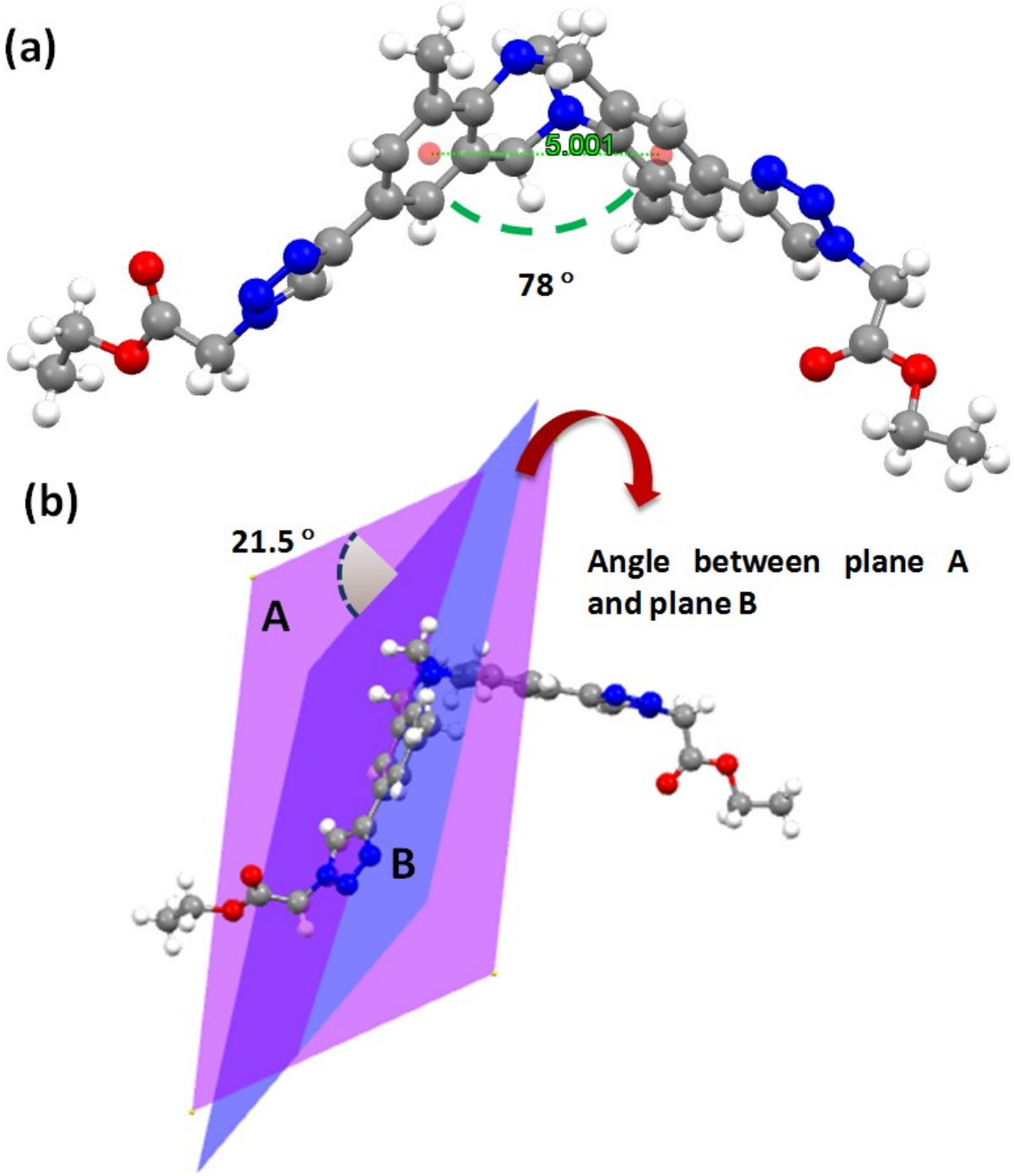

Figure S10. Crystal structure of TB-1 showing (a) distance between the phenyl rings of TB-core, (b) twist angle of triazole ring with respect to phenyl ring of TB-core.

Table S1: Crystal data of TB-1	
Crystal system	Monoclinic
Space group	P 21/c
a (Å)	12.312
b (Å)	34.200
c (Å)	13.951
α (deg)	90.00
β (deg)	104.87
γ (deg)	90.00
Volume ($Å^3$)	5677
Z	4
absorption coefficient (mm^{-1})	0.090
F(000)	2332
goodness-of-fit on F^2	0.863
Final *R* indices $[I > 2\sigma(I)]$	$R_1 = 0.0697$, $wR_2 = 0.1643$
R indices (all data)	$R_1 = 0.2025$, $wR_2 = 0.2176$

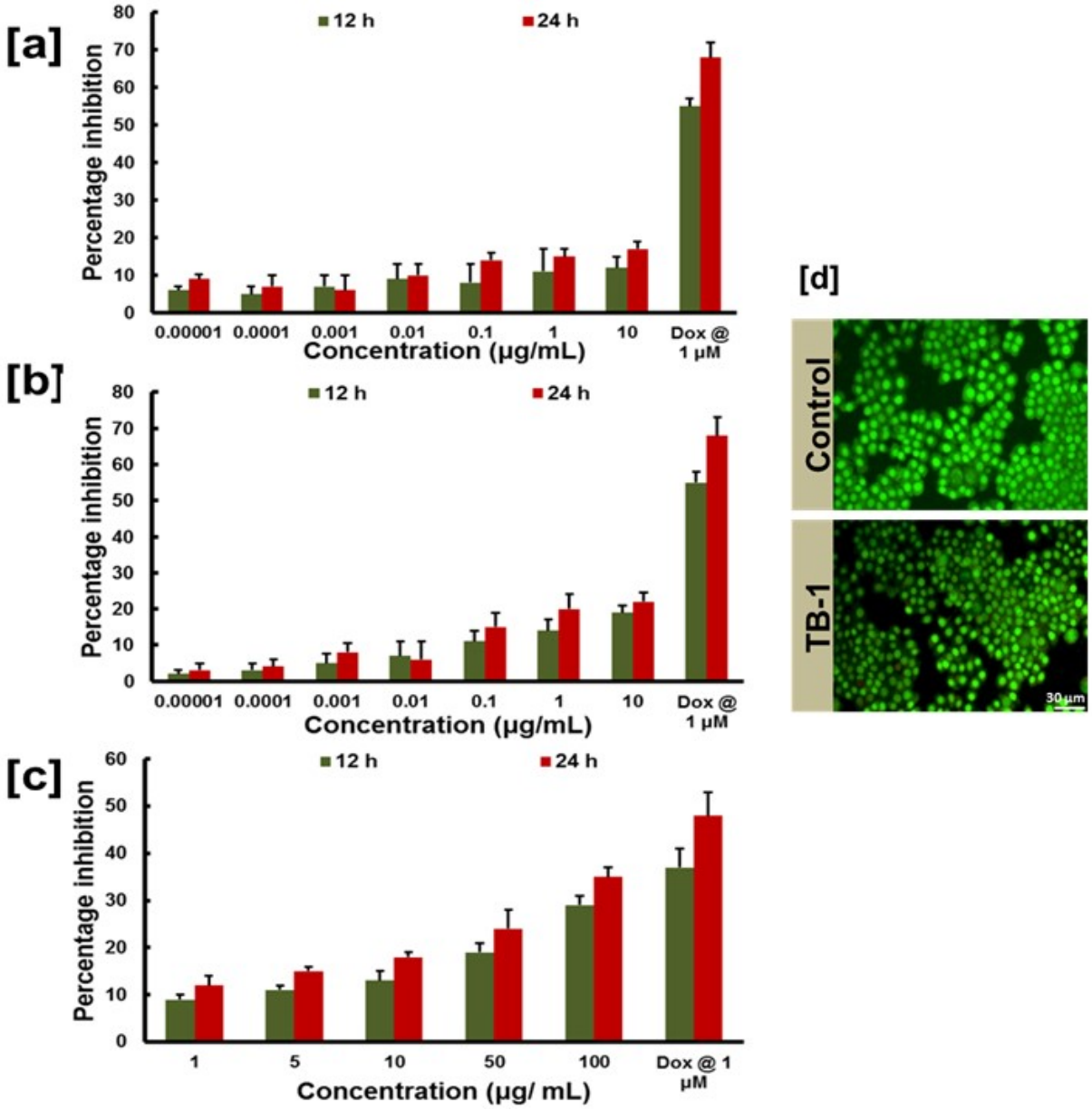

Figure S11. Evaluation of cytotoxicity of TB-1. Cytotoxicity of (a) HeLa, (b) A549, and (c) WI-38 by MTT assay. (d) Acridine orange-ethidium bromide staining on HeLa cells after the administration of TB-1 (10 μg/mL) for 24 h. Data represent mean ± SD from three independent experiments.

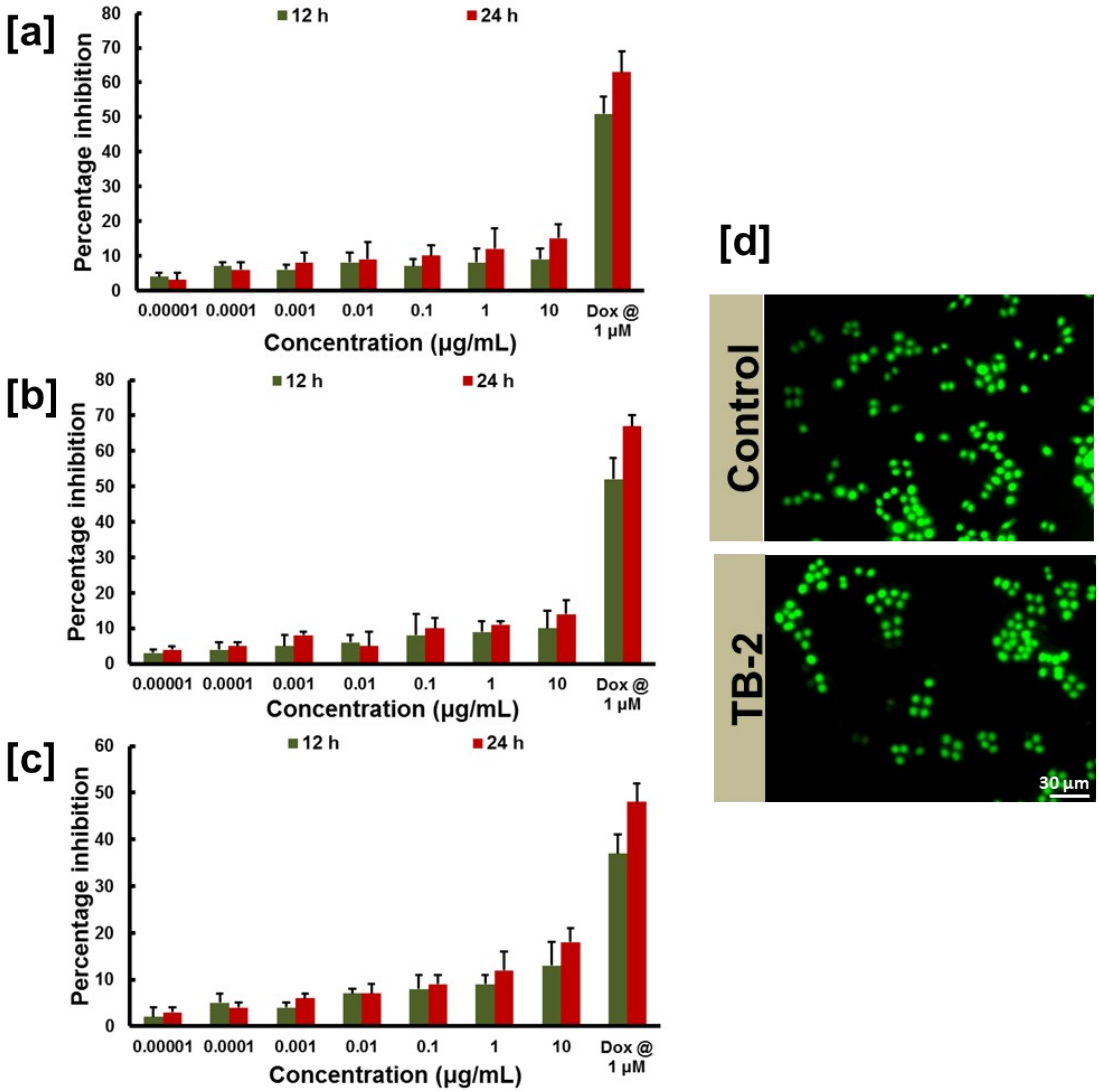

Figure S12. Evaluation of cytotoxicity of TB-2. Cytotoxicity of (a) HeLa, (b) A549, and (c) WI-38 by MTT assay. (d) Acridine orange-ethidium bromide staining on HeLa cells after the administration of TB-2 (10 μg/mL) for 24 h. The Data is mean ± SD representations from three independent experiments.

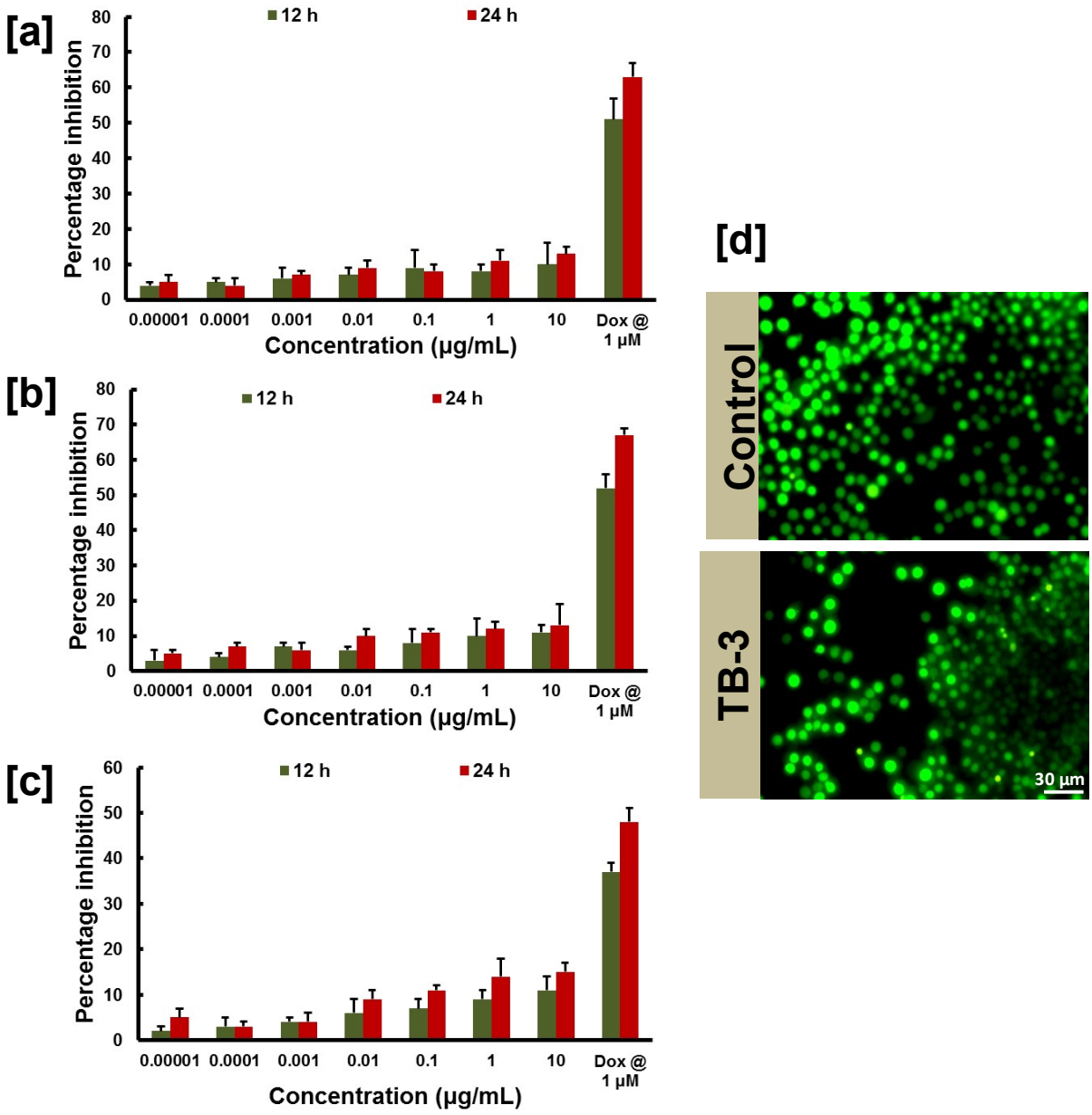

Figure S13. Evaluation of cytotoxicity of TB-3. Cytotoxicity of (a) HeLa, (b) A549, and (c) WI-38 by MTT assay. (d) Acridine orange-ethidium bromide staining on HeLa cells after the administration of TB-3 (10 μg/mL) for 24 h. The Data is mean ± SD representations from three independent experiments

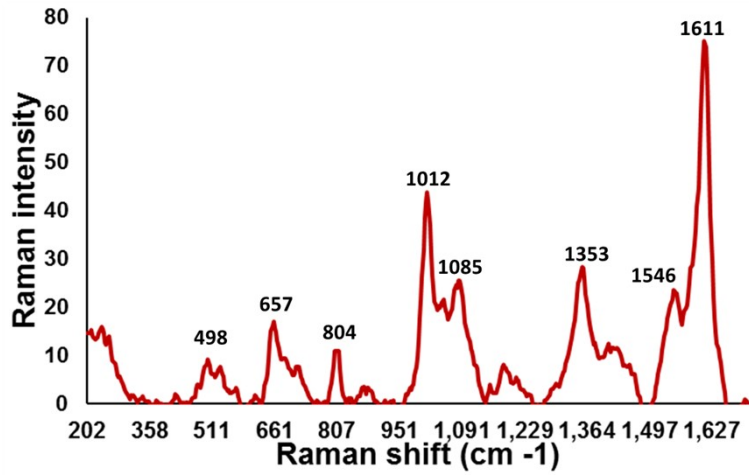

Figure S14. SERS Spectrum of TB-3 excited under 633 nm laser.

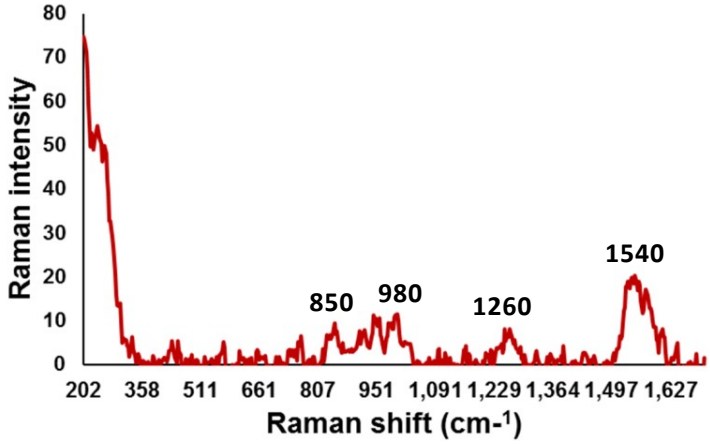

Figure S15. SERS Spectrum of ACE2 excited under 633 nm laser.

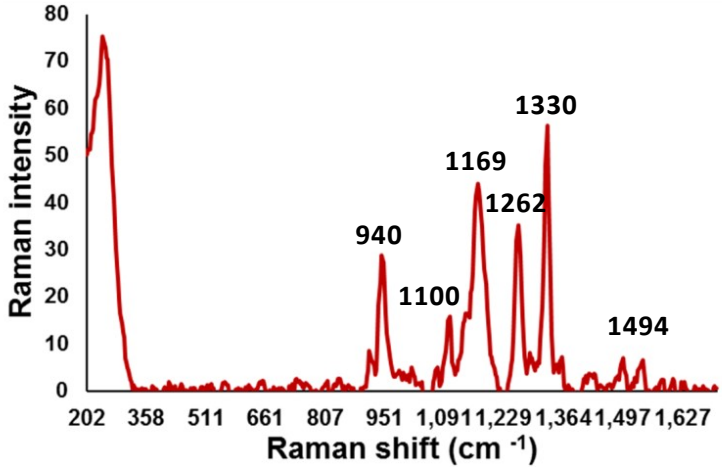

Figure S16. SERS Spectrum of SARS-CoV-2 Spike protein excited under 633 nm laser.

Table S2: SERS Peak assignment[5,6] for TB-3 excited with 633 nm laser.

Peak position (cm^{-1})	Peak assignment
1012	Aromatic ring breathing
1085	Aromatic ring breathing
1353	Triazole ring stretching
1546	Triazole ring stretching
1611	Benzene ring stretching, carboxylate stretching (C=O)

Table S3: SERS peak assignment[5,6] for ACE-2.

Peak position (cm^{-1})	Peak assignment
850	Single bond stretching vibrations for the amino acids and valine
980	C-C stretching of β-sheet (proteins)
1260	Amide III stretching and N-H bending
1540	Amide carbonyl group vibrations and aromatic hydrogens

Table S4: SERS peak assignment[5,6] for SARS-CoV-2 spike protein.

Peak position (cm^{-1})	Peak assignment
940	C-C skeletal stretching in protein
1100	Amide III and other groups (proteins)
1169	C-C/C-N stretching (proteins)
1262	Amide III stretching and N-H bending
1330	CH_3CH_2 wagging mode
1494	C-N stretching vibration coupled with the in-plane C-H bending in amino radical cations

Table S5: SERS peak assignment[5,6] for incubation of TB-3 (50 µg/mL) with ACE-2 (50 µg/mL).

Peak position (cm^{-1})	Peak assignment
1008	Phenylalanine, aromatic ring breathing
1359	Tryptophan, triazole ring stretching
1540	triazole ring stretching
1615	benzene ring stretching, carboxylate stretching (C=O)

Table S6: SERS peak assignment[5,6] for incubation of TB-3 (50 µg/mL) with SARS-CoV-2 spike protein (50 µg/mL).

Peak position (cm^{-1})	Peak assignment
662	C-S stretching mode of cystine (collagen type I)
1004	Phenylalanine (of collagen), phenyl breathing mode, n(C-C) phenylalanine
1200	Amide III- stretching and N-H bending
1544	triazole ring stretching
1614	carboxylate stretching (C=O), benzene ring stretching,

Table S7: SERS peak assignment [5,6] after co-incubation of TB-3 (50 µg/mL) with SARS-CoV-2 spike protein (50 µg/mL) and ACE2 (50 µg/mL) complex.

Peak position (cm^{-1})	Peak assignment
950	C-C skeletal stretching in protein
1096	Amide III and other groups (proteins)
1170	C-C/C-N stretching (proteins)
1260	Amide III stretching and N-H bending
1326	CH3CH2 wagging mode
1491	C-N stretching vibration coupled with the in-plane C-H bending in amino radical cations
1533	triazole ring stretching
1613	benzene ring stretching, carboxylate stretching stretching (C=O)

Table S8: Changes in SERS spectrum of TB-3 after co-incubation with ACE-2 and SARS-CoV-2 spike protein.

Changes in SERS spectrum (cm^{-1})	
TB-3	**TB-3 + ACE-2 + SARS-CoV-2**
1012	Peak broadened and shifted to 1007
1085	Peak broadened and shifted to 1075
1353	Peak broadened
1546	Peak shifted to 1533
1611	Peak intensity reduced

Table S9: Changes in SERS spectrum of ACE-2 after co-incubation with TB-3 and SARS-CoV-2 spike protein.

	Changes in SERS spectrum (cm^{-1})
ACE-2	**TB-3 + ACE-2 + SARS-CoV-2**
850	Peak intensity reduced and shifted to 840
980	Peak broadened
1260	The broad peak increased in intensity to a sharp peak
1540	The broad peak is converted to a sharp peak and merged with peak at 1533

Table S10: Changes in SERS spectrum of SARS-CoV-2 spike protein after co-incubation with TB-3 and ACE-2.

	Changes in SERS spectrum (cm^{-1})
SARS-Cov-2	**TB-3 + ACE-2 + SARS-COV-2**
940	Peak shifted to 950
1100	Peak shifted to1096
1169	Peak shifted to 1170
1262	Peak shifted to1260
1330	Peak shifted to1326
1494	Peak shifted to1491

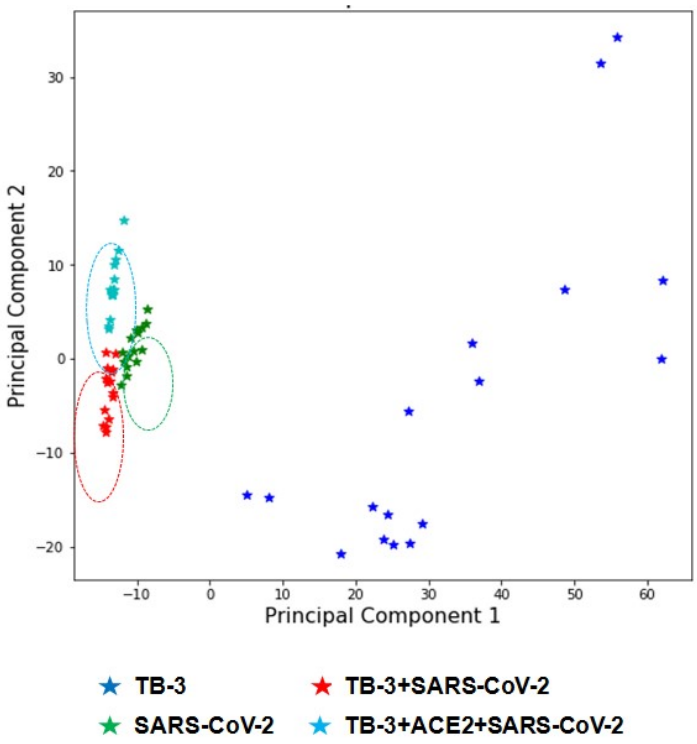

Figure S17. Two-component PCA of SERS studies for co-incubation of TB-3 with SARS-CoV-2 S-protein and ACE2.

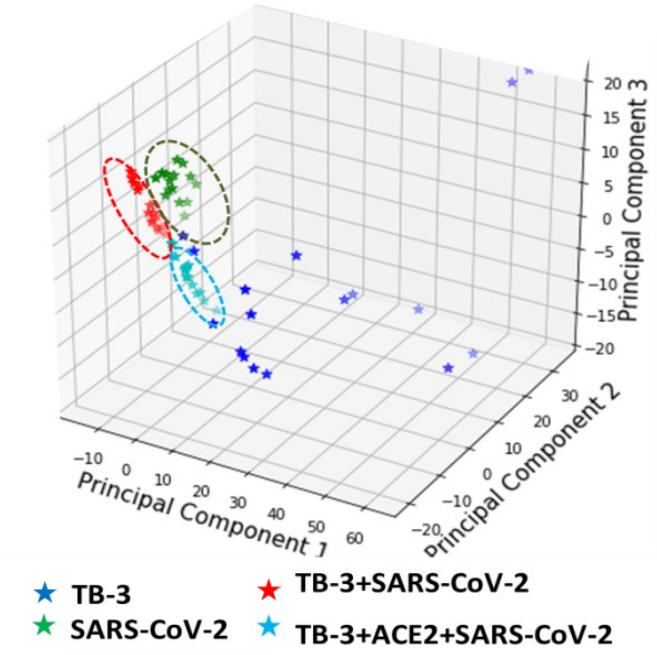

Figure S18. Three-component PCA of SERS studies for co-incubation of TB-3 with SARS-CoV-2 S-protein and ACE2.

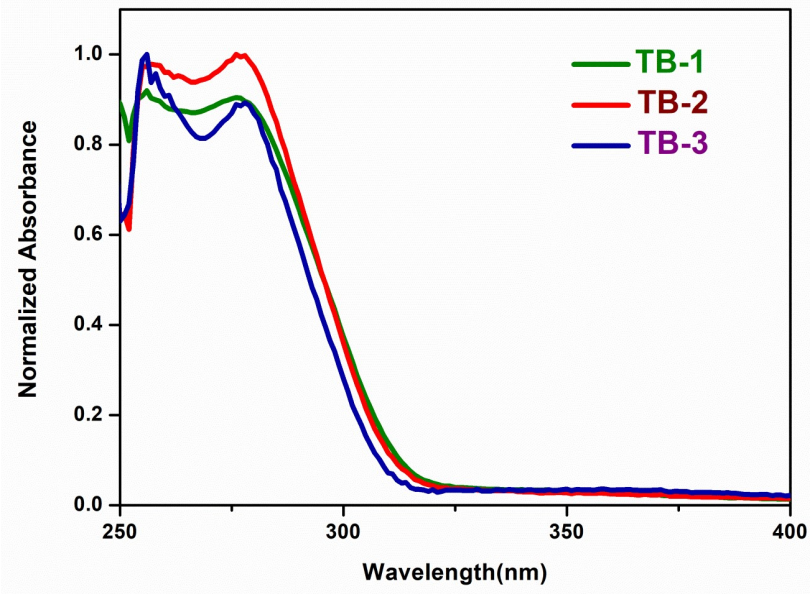

Figure S19. UV-Vis Absorption spectra of TBs.

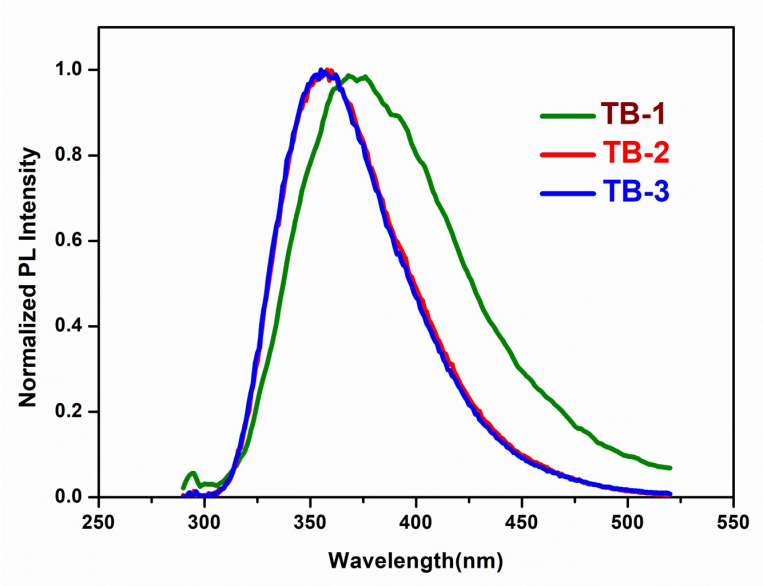

Figure S20. Fluorescence spectra of TBs.

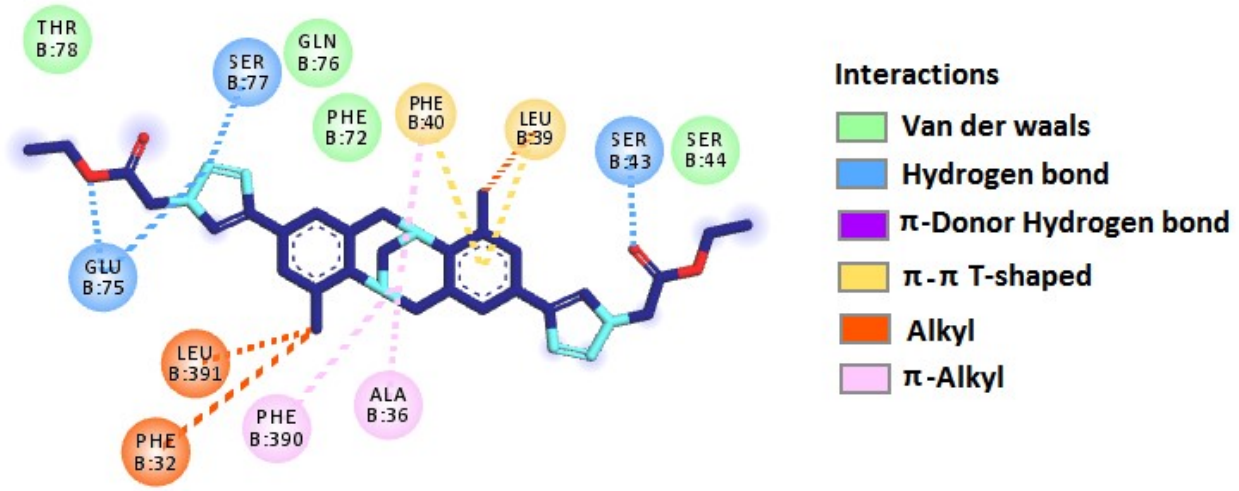

Figure S21. Types of intermolecular interactions between TB-1 and S-protein-ACE2 complex. Here, **A** and **B** represent amino acids of S-protein and ACE2, respectively.

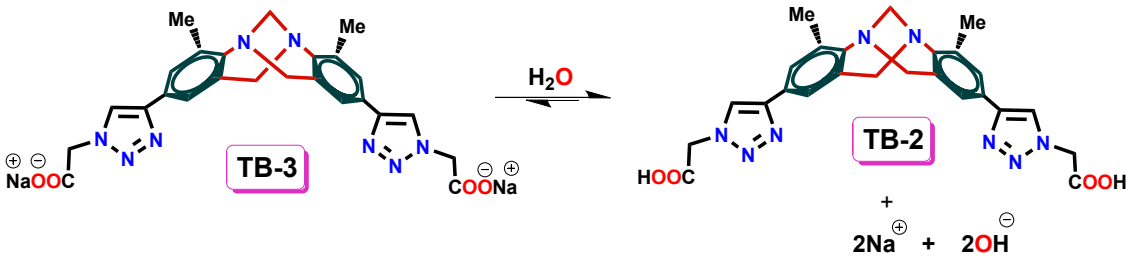

Figure S22. Equilibrium for dissociation of TB-3 in water.

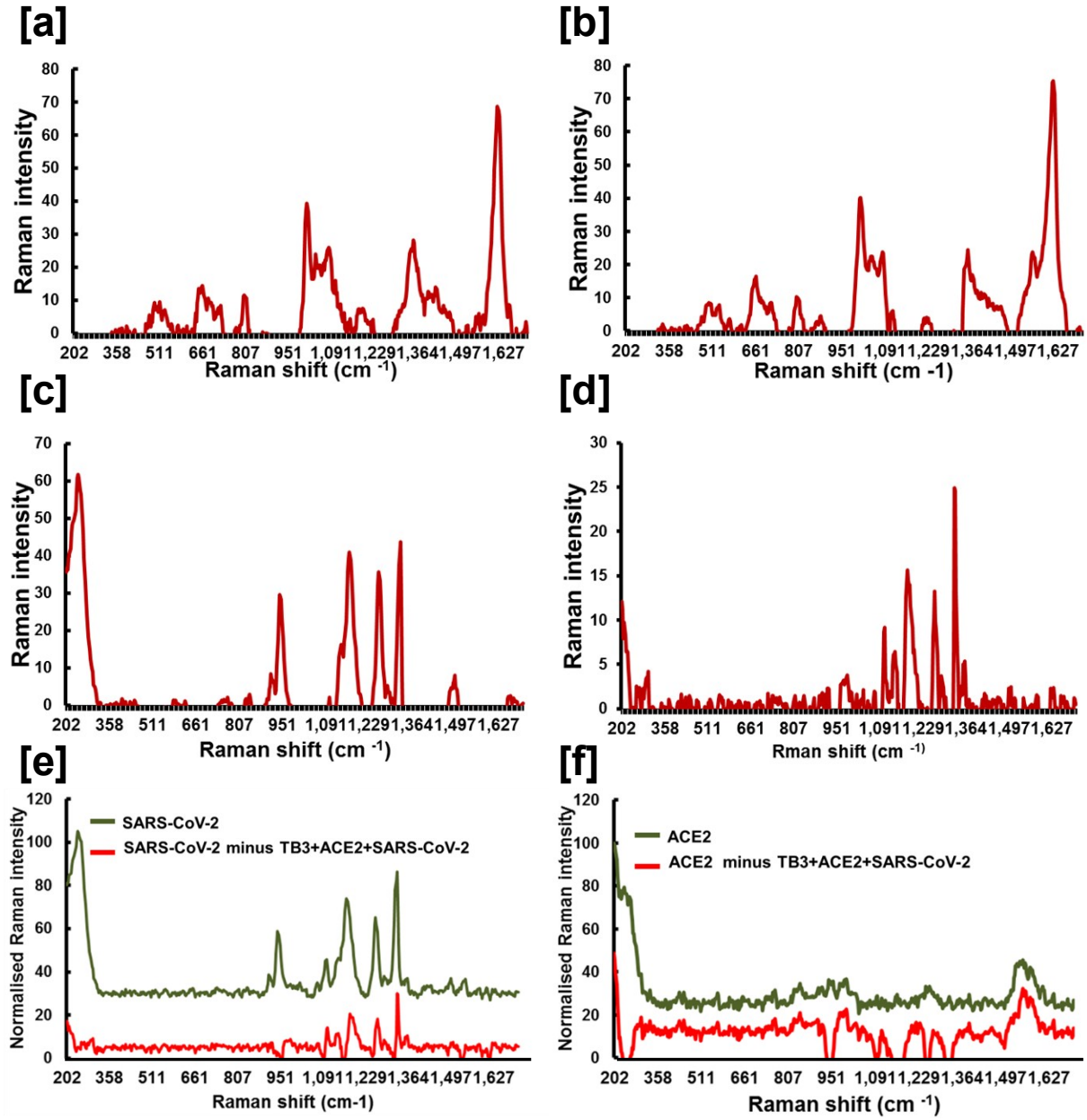

Figure S23. SERS spectral subtractions showing (a) TB-3 minus ACE2, (b) TB-3 minus SARS-CoV-2 S-protein, (c) SARS-CoV-2 S-protein minus TB-3, and (d) SARS-CoV-2 S-protein minus TB-3+ACE2+ SARS-CoV-2 S-protein. (e) Stacked spectrum of SARS-CoV-2 S-protein and SARS-CoV-2 S-protein minus TB-3+ACE2+ SARS-CoV-2. (f) Stacked spectrum of ACE2 and ACE2 minus TB-3+ACE2+ SARS-CoV-2.

References:

1. M. D. Smith and J. C. Smith, *ChemRxiv,* 2020, **2**, DOI: 10.26434/chemrxiv.11871402.v4.
2. M. M. Joseph, A. N. Ramya, V. M. Vijayan, J. B. Nair, B. T. Bastian and R. K. Pillai, *Small*, 2020, **16**, 1.
3. V. Karunakaran, V. N. Saritha, M. M. Joseph, J. B. Nair, G. Saranya, K. G. Raghu, K. Sujathan, K. S. Kumar and K. K. Maiti, *Nanomedicine Nanotechnology, Biol. Med*., 2020, **29**, 102276.
4. P. A. Lanza, D. Dusso, C. L. Ramirez, A. R. Parise, C. A. Chesta, E. L. Moyano and D. M. A. Vera, *European J. Org. Chem.,* 2019, **47**, 7644.
5. Z. Movasaghi, S. Rehman and I. U. Rehman, *Appl. Spectrosc. Rev.,* 2007, **42**, 493.
6. J. G. Grasselli and B. J. Bulkin (Eds.), *Analytical Raman Spectroscopy, Wiley, New York*, **1991**, 400.